

# Nonlinear Anderson localization in Toda lattices

Motohiko Ezawa

Department of Applied Physics, University of Tokyo, Hongo 7-3-1, 113-8656, Japan

We study the Anderson localization in nonlinear systems by taking a nonlinear transmission line realizing the Toda lattice. It is found that the randomness in inductance induces the Anderson localization in the voltage propagation. Furthermore, the nonlinearity enhances the Anderson localization. They are understood in terms of attractive interactions to form a soliton in a nonlinear system. Our results will be applicable in general to the Anderson localization in nonlinear systems that have solitons.

## I. INTRODUCTION

The Anderson localization is a prominent phenomenon inherent to disordered systems<sup>1</sup>, where the system exhibits an insulating behavior due to disorders. It is caused by the interference of wave functions due to multiple-scattering paths under a random potential. In the strong scattering limit, the wave functions are completely trapped by a disordered medium. The Anderson localization has been discussed in various systems<sup>2-5</sup> including nonlinear systems<sup>6,7</sup>. It is pointed out that the Anderson localization is destructed due to a nonlinearity in the case of the discrete Anderson nonlinear Schrödinger equation<sup>7</sup>. On the other hand, the enhancement and delocalization of the Anderson localization are reported in photonic lattices<sup>6</sup>. It is an intriguing problem to make a further investigation how the nonlinearity affects the Anderson localization.

Electric circuits attract renewed interest in the context of topological physics<sup>8-22</sup> based on the observation that a circuit Laplacian may be identified with a Hamiltonian. Furthermore, the telegrapher equation is rewritten in the form of the Schrödinger equation, and thus describes the behavior of a quantum walker<sup>23-25</sup>. One of the merits of electric circuits is that we can naturally introduce nonlinear elements into circuits. Hence, electric circuits present an ideal playground to study nonlinear physics. There are also some studies on topological physics in nonlinear electric circuits<sup>26-28</sup>.

The Toda lattice is a celebrated nonlinear exactly solvable model possessing soliton solutions<sup>29-31</sup>. It is realized in a nonlinear transmission line consisting of variable capacitance diodes and inductors<sup>32-38</sup>, as illustrated in Fig.1(a). Recently, it is shown that the dimerized Toda lattice has a topological phase<sup>28</sup> which is a nonlinear extension of the Su-Schrieffer-Heeger model.

In this paper, we study an interplay between the Anderson localization and nonlinear effects taking an instance of a nonlinear transmission line realizing the Toda lattice. We introduce randomness into the inductance of the transmission line and investigate the dynamics of the voltage propagation starting from one node. Namely, we analyze a propagation dynamics of the voltage by giving a delta-function type pulse at one node. The diffusion process strongly depends on the strength of the disorder. It is found that the voltage propagation shows a localization behavior when disorders are strong enough, which is the nonlinear Anderson localization in the nonlinear transmission line. Furthermore, it is found that the nonlinearity enhances the Anderson localization.

We interpret these phenomena as caused by the presence

of the attractive nonlinear force in a nonlinear system which has a soliton. Indeed, in a soliton system, there is an attractive force in order to prevent a soliton from decaying. Without the attractive force, the waves with the different momenta propagate with different velocities, resulting in the destruction of a soliton. This attractive force maintains the wave packet starting from the delta function even though it is not a soliton solution. Moreover, once one of the wave components is trapped to a randomness, the other components are also trapped, which enhances the localization in the nonlinear system. Then, it is natural that the localization is strong when the nonlinearity is strong. Our results will be applicable in general to the nonlinear Anderson localization in nonlinear systems having solitons.

## II. TODA LATTICE

We review the Toda model. The Toda Hamiltonian is defined by<sup>29,30</sup>

$$H = \sum_n \frac{m}{2} \left( \frac{dy_n}{dt} \right)^2 + \Phi(r_n), \quad (1)$$

where  $r_n = y_{n+1} - y_n$ , and  $\Phi(r_n)$  is the Toda potential,

$$\Phi(r_n) \equiv \frac{a}{b} e^{-br_n} + ar_n - \frac{a}{b}. \quad (2)$$

A nonlinear differential equation follows from Eq.(1),

$$m \frac{d^2 y_n}{dt^2} = f_{n-1} - f_n, \quad (3)$$

where  $f_n$  is the force,

$$f_n = -\frac{d}{dr_n} \Phi(r_n). \quad (4)$$

The Toda equation (3) is rewritten in the form of

$$m \frac{d^2}{dt^2} \log \left( 1 + \frac{f_n}{a} \right) = b(f_{n+1} + f_{n-1} - 2f_n), \quad (5)$$

which is well realized by a transmission line with variable-capacitance diodes<sup>32</sup>. See Fig.1(a) and Eq.(15).

The right hand side of Eq.(5) is identical to the tight-binding hopping Hamiltonian between the nearest neighbor sites,

$$H = \sum_n M_{nm} |\psi_n\rangle \langle \psi_m|, \quad (6)$$

where  $M_{nm} = b(\delta_{n-1,m} + \delta_{n+1,m} - 2\delta_{nm})$  with  $b$  the hopping parameter.

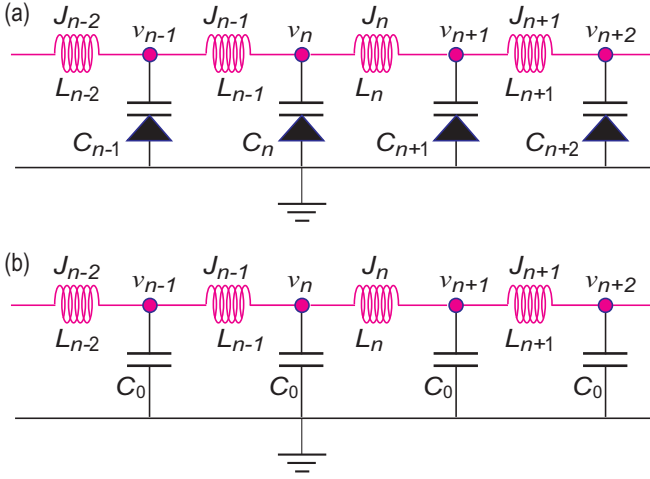


FIG. 1: Illustration of a transmission line made of (a) nonlinear elements realizing the inhomogeneous Toda lattice and (b) linear elements realizing the telegrapher equation. The inductance indicated by magenta is random. Each node is grounded via a variable-capacitance diode and a capacitor in (a) and (b), respectively.

### III. INHOMOGENEOUS TODA LATTICE

We generalize the Toda lattice to an inhomogeneous Toda lattice<sup>28</sup>, because the hopping becomes node-dependent in the presence of randomness in the transmission line. We show the transmission line corresponding to the inhomogeneous Toda lattice in Fig.1(a), which consists of variable-capacitance diodes and inductors. The Kirchhoff law is given by

$$L_n \frac{dJ_n}{dt} = v_n - v_{n+1}, \quad (7)$$

$$\frac{dQ_n}{dt} = J_{n-1} - J_n, \quad (8)$$

where  $v_n$  is the voltage,  $J_n$  is the current and  $Q_n$  is the charge at the node  $n$ , while  $L_n$  is the inductance for the inductor between the nodes  $n$  and  $n+1$ , as illustrated in Fig.1(a). The Kirchhoff law is summarized in the form of the second-order differential equation,

$$\begin{aligned} \frac{d^2 Q_n}{dt^2} &= \frac{dJ_{n-1}}{dt} - \frac{dJ_n}{dt} \\ &= \frac{1}{L_{n-1}} (V_{n-1} - V_n) - \frac{1}{L_n} (V_n - V_{n+1}), \end{aligned} \quad (9)$$

where we have introduced a new variable  $V_n$  by  $v_n = V_0 + V_n$ .

The capacitance is a function of the voltage  $V_n$  in the variable-capacitance diode, and it is well given by<sup>33</sup>

$$C(V_n) = \frac{Q(V_0)}{F_0 + V_n - V_0}, \quad (10)$$

where  $F_0$  is a constant characteristic to the variable-capacitance diode. Especially, we have

$$C(V_0) = \frac{Q(V_0)}{F_0}. \quad (11)$$

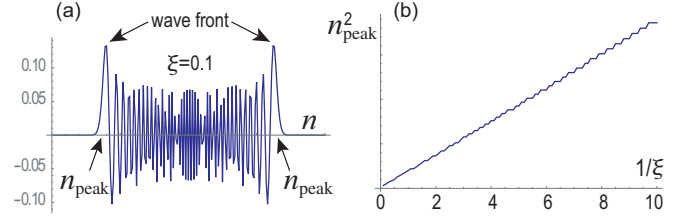


FIG. 2: (a) Wave pattern of the voltage  $V_n$  at a fixed time  $t$  with  $\xi = 0.1$ . The vertical axis is the voltage in the unit of  $V_1$ . (b)  $n_{\text{peak}}^2$  as a function of the nonlinearity  $\xi$  at a fixed time  $t$ . We have set  $Q(V_0) = L = 1$ .

The charge is given by

$$\begin{aligned} Q_n &= \int_0^{V_n} C(V) dV \\ &= Q(V_0) \log \left[ 1 + \frac{V_n}{F_0} \right] + \text{const.} \end{aligned} \quad (12)$$

A closed form of the differential equation for  $V_n$  follows from Eqs.(9) and (12),

$$\begin{aligned} Q(V_0) \frac{d^2}{dt^2} \log \left[ 1 + \xi \frac{V_n}{V_1} \right] \\ = \frac{V_{n+1}}{L_n} - \left( \frac{1}{L_{n-1}} + \frac{1}{L_n} \right) V_n + \frac{V_{n-1}}{L_{n-1}}, \end{aligned} \quad (13)$$

where we have introduced a dimensionless nonlinearity parameter

$$\xi \equiv V_1/F_0. \quad (14)$$

Small  $\xi$  implies weak nonlinearity, while large  $\xi$  implies strong nonlinearity. It is an inhomogeneous generalization of the Toda equation.

We first study the homogeneous case  $L_n = L$ . Eq.(13) is reduced to

$$Q(V_0) \frac{d^2}{dt^2} \log \left[ 1 + \xi \frac{V_n}{V_1} \right] = \frac{1}{L} (V_{n+1} - 2V_n + V_{n-1}), \quad (15)$$

which is the Toda equation (5) with  $m = Q(V_0)$ ,  $a = F_0$  and  $b = 1/L$ . We set an initial condition,

$$V_n(0) = V_1 \delta_{n,n_1}, \quad (16)$$

where the voltage is nonzero only at the node  $n_1$ .

The Toda equation (15) is reduced to a linear wave equation by taking the limit  $\xi \rightarrow 0$  in (10),

$$C(V_0) \frac{d^2 V_n}{dt^2} = \frac{1}{L} (V_{n+1} - 2V_n + V_{n-1}). \quad (17)$$

Correspondingly, a nonlinear transmission line [Fig.1(a)] is reduced to a linear transmission line [Fig.1(b)], which we have already studied in the context of quantum walks<sup>23</sup>.

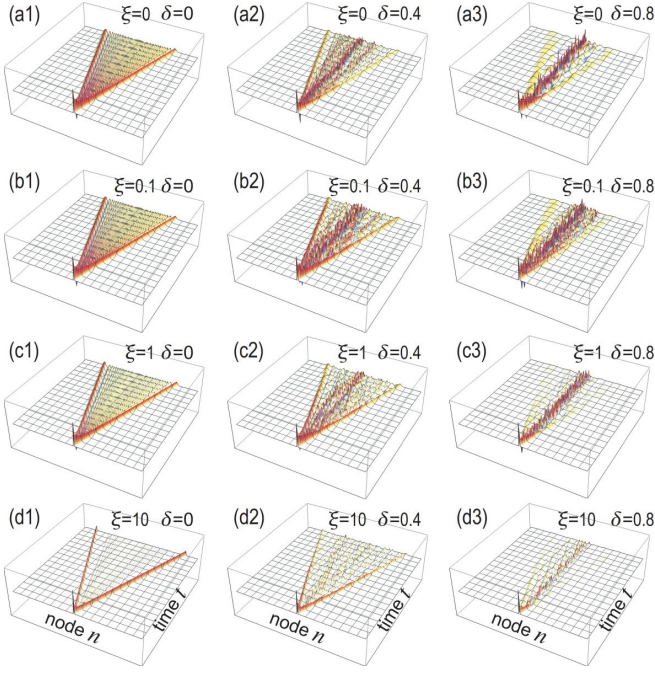


FIG. 3: Dynamics of the voltage propagation. (a1)~(d1)  $\delta = 0$ , (a2)~(d2)  $\delta = 0.4$ , and (a3)~(d3)  $\delta = 0.8$ . (a1)~(a3) Linear wave propagation corresponding to  $\xi = 0$ . We have set (b1)~(b3)  $\xi = 0.1$ , (c1)~(c3)  $\xi = 1$  and (d1)~(d3)  $\xi = 10$ . The vertical axis is the dimensionless voltage  $x_n$ .

#### IV. DYNAMICS OF THE VOLTAGE PROPAGATION

We investigate the time evolution of the voltage  $V_n$  by solving the Toda equation (15) numerically together with the initial condition (16). In Fig.2(a), we show the wave pattern of  $V_n$  as a function of the node  $n$  at a fixed time, where the absolute value of the voltage takes the largest value at the wave front whose position is indicated by  $n_{\text{peak}}$ . In Fig.3(a1), (b1), (c1) and (d1), we show the time evolution of the voltage propagation for  $\xi = 0, 0.1, 1$  and  $10$ , respectively. It shows a diffusive motion of a wave, where the wave front is indicated in red. It is found to be a linear function of the time  $t$ ,  $n_{\text{peak}} \propto t$ . Next, we have plotted the peak position  $n_{\text{peak}}^2$  as a function of  $\xi^{-1}$  with all other variables fixed in Fig.2(b). It is clearly a linear function of  $\xi^{-1}$ , or  $n_{\text{peak}} \propto \xi^{-1/2}$ . Consequently, it follows that

$$n_{\text{peak}} \propto \xi^{-1/2} t \propto \sqrt{F_0} t, \quad (18)$$

when  $L$  and  $Q(L_0)$  are fixed.

We note that the ripples are confined between two wave fronts and absent outside of the wave fronts. This resembles the light cone, where the information propagates with a finite velocity.

A prominent feature of the wave pattern reads as follows: There are many ripples between two wave fronts in Fig.3(a1) and (b1). In particular, Fig.3(a1) is for the voltage propagation in the linear limit, where the delta-function like pulse disperses quickly because its Fourier components propagate

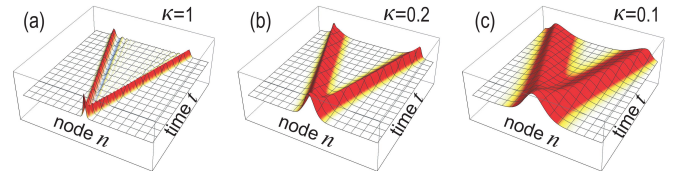


FIG. 4: Propagation dynamics of the Toda soliton. (a)  $\kappa = 1$ , (b)  $\kappa = 0.2$  and (c)  $\kappa = 0.1$ . The vertical axis is the voltage  $V_n$ . We have set  $C(V_0) = 0.1$  and  $L = F_0 = 1$ .

freely. This is approximately the case provided the nonlinearity is weak as in Fig.3(b1) or in Fig.2(a). On the other hand, the ripples are weak and the two wave fronts look as if they are two isolated solitary waves in strong nonlinear systems as in Fig.3(d1).

#### V. TODA SOLITON SOLUTION

It is well known that the Toda equation (15) has an exact soliton solution. By assuming the Toda soliton starts from  $n = 1$  at  $t = 0$ , it is given by<sup>29-31</sup>

$$V_n = F_0 \sinh^2 \kappa \operatorname{sech}^2 (\kappa n - \beta t), \quad (19)$$

where

$$\beta = \pm \sqrt{\frac{F_0}{LQ(V_0)}} \sinh \kappa = \pm \frac{1}{\sqrt{LC(V_0)}} \sinh \kappa, \quad (20)$$

and  $\kappa$  is a constant determining the width of the soliton. In Fig.4, we show the time evolution of the voltage  $V_n$  subject to the Toda equation (15) for various  $\kappa$ . The soliton splits into two solitons and propagate in two directions without tails.

It follows from Eq.(19) that the position  $n_{\text{Toda}}$  of the Toda soliton moves as

$$n_{\text{Toda}} = \frac{\beta}{\kappa} t = \pm \sqrt{\frac{1}{LQ(V_0)}} \frac{\sinh \kappa}{\kappa} \sqrt{F_0} t, \quad (21)$$

which is consistent with Eq.(18).

Let us make a qualitative argument with respect to the propagations of the wave front and the Toda soliton. First, it is found that the propagation of the Toda soliton for  $\kappa = 1$  in Fig.4(a) is quite similar to that of the wave front for  $\xi = 10$  in Fig.3(d1). It seems that the Toda soliton becomes the delta-function type as  $\kappa \rightarrow \infty$ , while the wave front becomes the delta-function type as  $\xi \rightarrow \infty$ .

Indeed, when the soliton width is small enough, we may approximate Eq.(19) as

$$V_n = 2F_0 \sinh^2 \kappa \delta(\kappa n - \beta t). \quad (22)$$

The narrow soliton corresponds to the limit  $\kappa \rightarrow \infty$ , which corresponds to the limit  $\xi \rightarrow \infty$  to keep the voltage finite.

We summarize our observation with respect to the voltage propagation in Fig.3(b1)~(d1) as follows. In a soliton system,

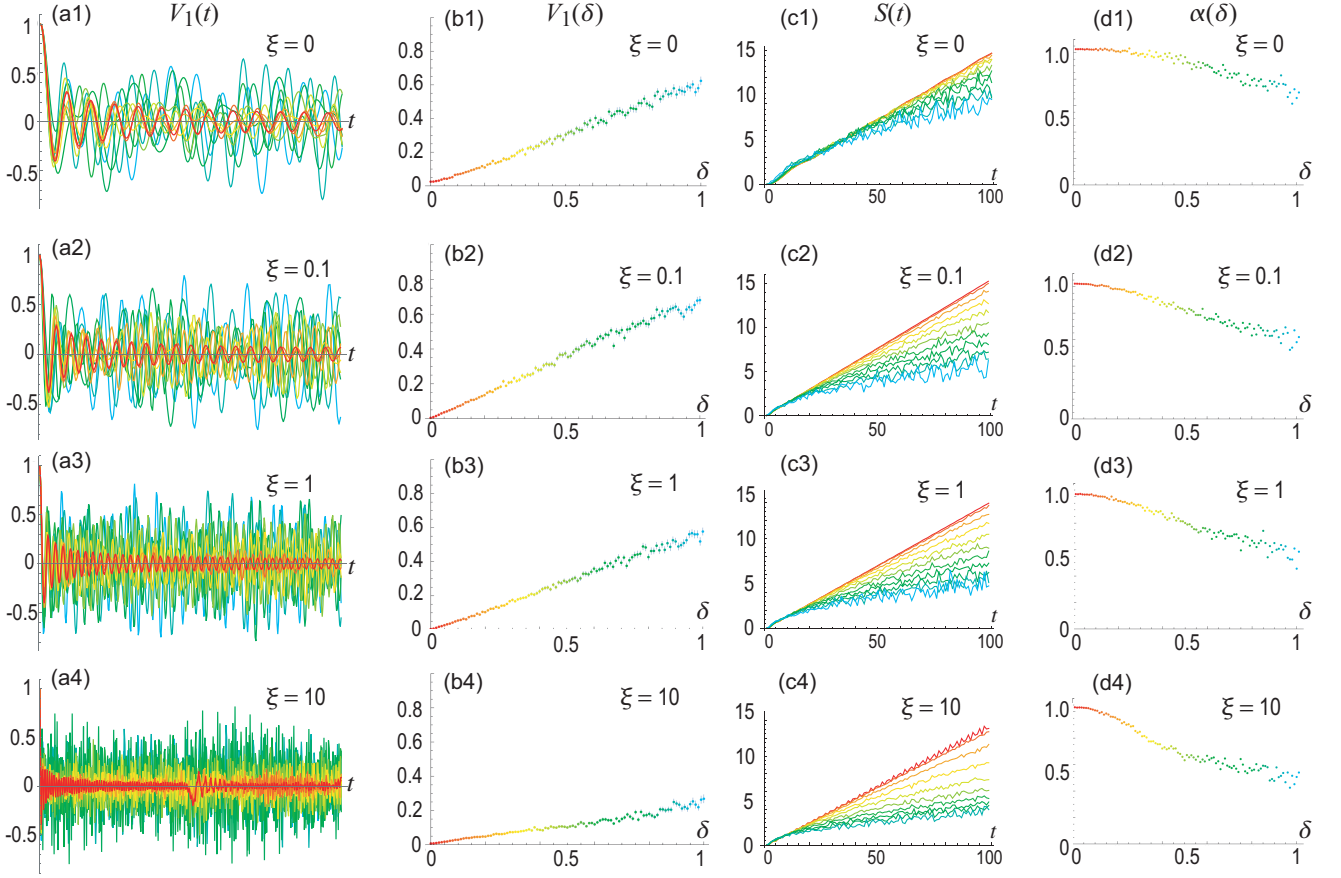


FIG. 5: (a1)~(a4) Time evolution of the voltage at the initial node  $n_1$ . The vertical axis is the voltage in the unit of  $V_1$ . (b1)~(b4) The voltage at the initial node after enough time. Red color indicates  $\delta = 0$ , while cyan color indicates  $\delta = 1$ . (c1)~(c4) 100 times average of time evolution of the standard deviation  $S(t)$  for various disorder strength  $\delta$  in the unit of  $V_1$ . (d1)~(d4) The fitted standard deviation exponent  $\alpha$  as a function of disorder strength  $\delta$ . (a1)~(d1) Linear wave ( $\xi = 0$ ). We have set (a2)~(d2)  $\xi = 0.1$ , (a3)~(d3)  $\xi = 1$  and (a4)~(d4)  $\xi = 10$ . We have set  $C(V_0) = 0.1$  and  $L = 1$ .

there is an attractive force in order to form a soliton. Without the attractive force, the waves with the different momenta propagate with different velocities, resulting in the destruction of a soliton. This attractive force maintains the wave packet starting from the delta function even though it is not a soliton solution.

## VI. EFFECTS OF RANDOMNESS

We introduce randomness into inductors uniformly distributing from  $-\delta$  to  $\delta$ . As a result the inductance  $L$  becomes node-dependent,  $L \rightarrow L_n$ , where

$$L_n = L(1 + \eta_n \delta), \quad (23)$$

with  $\eta_n$  being a random variable ranging from  $-1$  to  $1$ . Typical values are  $\delta = 0.05 \sim 0.2$  in electric circuits.

We now solve the inhomogeneous Toda equation (13) with the use of Eq.(23). We show the time evolution of the voltage for various  $\delta$  and  $\xi$  in Fig.3. We show the results with  $\delta = 0.4$  in Fig.3(a2)~(d2), where there remains a localized

component at the initial node  $n_1$  although the wave fronts are clearly seen. The voltage is almost localized at the initial node  $n_1$  for  $\delta = 0.8$ , as shown in Fig.3(a3)~(d3).

Next we show the time evolution of the voltage at the initial node  $n_1$  for various  $\xi$  in Fig.5(a1)~(a4). The voltage rapidly decreases in the absence of the disorder, as shown by the red curves ( $\delta = 0$ ). The voltage can be checked to vanish after enough time, although such a limit is not displayed in these figures. On the other hand, the voltage remains nonzero when the disorder is introduced as indicated by cyan curves ( $\delta = 1$ ). We plot the voltage after enough time in Fig.5(b1)~(b4). The remnant voltage is almost proportional to the disorder strength  $\delta$ . We note that there is no significant dependence on  $\xi$ .

We define the standard deviation of the voltage propagation by

$$S(t) \equiv \sqrt{\sum_n (n - n_1)^2 V_n^2(t)}, \quad (24)$$

where  $n_1$  is the initial node. We show the time evolution of the standard deviation in Fig.5(c1)~(c4). It increases almost linearly as a function of the time. It indicates a diffusion

process of the quantum-walk type. We approximate  $S(t)$  by  $S(t) \propto t^\alpha$  as a function of  $t$ . We show the exponent  $\alpha$  in Fig.5(d1)~(d4). It is almost constant  $\alpha = 1$  for  $\delta < 0.4$  for  $\xi = 0$  and  $\delta < 0.1$  for  $\xi = 0.1, 1, 10$ , while it decreases gradually as the increase of  $\delta$ . The exponent  $\alpha$  decreases rapidly to  $\alpha \simeq 0.5$  for strong nonlinearity  $\xi$ , as shown in Fig.5(d4). It indicates that the nonlinearity enhances the Anderson localization.

## VII. DISCUSSION

We discuss why the Anderson localization enhances in the nonlinear system with the Toda soliton. In the linear wave equation, the waves with the different momenta propagate independently. On the other hand, the waves do not propagate independently in nonlinear wave equations. Especially, there is such an interaction in a soliton system that prohibits the soliton from decaying. Hence, there must be a strong attractive force preventing a solitary wave from diffusing. We interpret

this phenomenon as caused by the presence of the attractive nonlinear force forming a soliton in the Toda model. Once one of the wave components is trapped to a randomness, the other components are also trapped, which enhances the localization in the nonlinear system. Furthermore, the localization is stronger when the nonlinearity is stronger. Our results will be applicable to the nonlinear Anderson localization in other soliton systems. It is interesting to study the Anderson localization in other nonlinear systems.

In conclusion, we have studied nonlinear Anderson localization in Toda lattices, where we find that the nonlinearity enhances the localization. Our results will excite further studies on the relevance of the nonlinearity to the Anderson localization.

The author is very much grateful to M. Kawamura, S. Katsumoto and N. Nagaosa for helpful discussions on the subject. This work is supported by the Grants-in-Aid for Scientific Research from MEXT KAKENHI (Grants No. JP17K05490 and No. JP18H03676). This work is also supported by CREST, JST (JPMJCR16F1 and JPMJCR20T2).

- 
- <sup>1</sup> P. W. Anderson, Phys. Rev. **109**, 1492 (1958)
  - <sup>2</sup> M. Cutler and N. F. Mott, Phys. Rev. **181**, 1336 (1969)
  - <sup>3</sup> T. Giamarchi and H. J. Schulz, Phys. Rev. B **37**, 325 (1988)
  - <sup>4</sup> G. Roati, C. D'Errico, L. Fallani, M. Fattori, C. Fort, M. Zaccanti, G. Modugno, M. Modugno and M. Inguscio, Nature **453**, 895 (2008)
  - <sup>5</sup> M. Segev, Y. Silberberg and D. N. Christodoulides, Nature Photonics **7**, 197 (2013)
  - <sup>6</sup> Y. Lahini, A. Avidan, F. Pozzi, M. Sorel, R. Morandotti, D. N. Christodoulides, Y. Silberberg, Phys. Rev. Lett. **100**, 013906 (2008)
  - <sup>7</sup> A. S. Pikovsky and D. L. Shepelyansky, Phys. Rev. Lett. **100**, 094101 (2008)
  - <sup>8</sup> S. Imhof, C. Berger, F. Bayer, J. Brehm, L. Molenkamp, T. Kiessling, F. Schindler, C. H. Lee, M. Greiter, T. Neupert, R. Thomale, Nat. Phys. **14**, 925 (2018).
  - <sup>9</sup> C. H. Lee, S. Imhof, C. Berger, F. Bayer, J. Brehm, L. W. Molenkamp, T. Kiessling and R. Thomale, Communications Physics, **1**, 39 (2018).
  - <sup>10</sup> T. Helbig, T. Hofmann, C. H. Lee, R. Thomale, S. Imhof, L. W. Molenkamp and T. Kiessling, Phys. Rev. B **99**, 161114 (2019).
  - <sup>11</sup> Y. Lu, N. Jia, L. Su, C. Owens, G. Juzeliunas, D. I. Schuster and J. Simon, Phys. Rev. B **99**, 020302 (2019).
  - <sup>12</sup> K. Luo, R. Yu and H. Weng, Research (2018), ID 6793752.
  - <sup>13</sup> E. Zhao, Ann. Phys. **399**, 289 (2018).
  - <sup>14</sup> Y. Li, Y. Sun, W. Zhu, Z. Guo, J. Jiang, T. Kariyado, H. Chen and X. Hu, Nat. Com. **9**, 4598 (2018)
  - <sup>15</sup> M. Ezawa, Phys. Rev. B **98**, 201402(R) (2018).
  - <sup>16</sup> M. Serra-Garcia, R. Susstrunk and S. D. Huber, Phys. Rev. B **99**, 020304 (2019).
  - <sup>17</sup> T. Hofmann, T. Helbig, C. H. Lee, M. Greiter, R. Thomale, Phys. Rev. Lett. **122**, 247702 (2019).
  - <sup>18</sup> M. Ezawa, Phys. Rev. B **100**, 045407 (2019).
  - <sup>19</sup> M. Ezawa, Phys. Rev. B **99**, 201411(R) (2019).
  - <sup>20</sup> M. Ezawa, Phys. Rev. B **99**, 121411(R) (2019).
  - <sup>21</sup> M. Ezawa, Phys. Rev. B **102**, 075424 (2020).
  - <sup>22</sup> C. H. Lee, T. Hofmann, T. Helbig, Y. Liu, X. Zhang, M. Greiter and R. Thomale, Nature Communications **11**, 4385 (2020).
  - <sup>23</sup> M. Ezawa, Phys. Rev. B **100**, 165419 (2019).
  - <sup>24</sup> M. Ezawa, Phys. Rev. Research **2**, 023278 (2020).
  - <sup>25</sup> M. Ezawa, J. Phys. Soc. Jpn. **89**, 124712 (2020).
  - <sup>26</sup> T. Kotwal, H. Ronellenfitsch, F. Moseley, A. Stegmaier, R. Thomale, J. Dunkel, arXiv:1903.10130
  - <sup>27</sup> K. Sone, Y. Ashida, T. Sagawa, arXiv:2012.09479
  - <sup>28</sup> M. Ezawa, arXiv:2105.10851
  - <sup>29</sup> M. Toda, J. Phys. Soc. Jpn. **22**, 431 (1967).
  - <sup>30</sup> M. Toda, Springer Ser. Solid State Sci. **20**, Springer, Berlin, (1981).
  - <sup>31</sup> M. Toda, Proc. Jpn. Acad. Ser. B **80**, 445 (2004).
  - <sup>32</sup> R. Hirota and K. Suzuki, J. Phys. Soc. Jpn. **28**, 1366 (1970).
  - <sup>33</sup> H. Nagashima and Y. Amagishi, J. Phys. Soc. Jpn. **45**, 680 (1978).
  - <sup>34</sup> A. C. Singer and A. V. Oppenheim, Int. J. Bifurcation and Chaos **09**, 571 (1999)
  - <sup>35</sup> D. Yemele, P. Marquie and J. Marie Bilbault, Phys. Rev. E **68**, 016605 (2003)
  - <sup>36</sup> D. Yemele, P. K. Talla and T. C. Kofané, J. Phys. D: Appl. Phys. **36**, 1429 (2003)
  - <sup>37</sup> F. B. Pelap and M. M. Faye, J. Math. Phys. **46**, 033502 (2005)
  - <sup>38</sup> A. Houwe, S. Abbagari, M. Inc, G. Betchewe, S. Y. Doka, K. T. Crepin, K.S. Nisar, Results in Physics **18**, 203188 (2020)